

Supporting Information

Simulation Investigation of the Spontaneous Motion Behaviors of Underwater Oil Droplets on Conical Surface

Chaolang Chen*, Jian Liu, Yangkai Liu, Xuqiao Peng

School of Mechanical Engineering, Sichuan University, Chengdu 610065, PR China

*Corresponding author: chaolangchen@scu.edu.cn

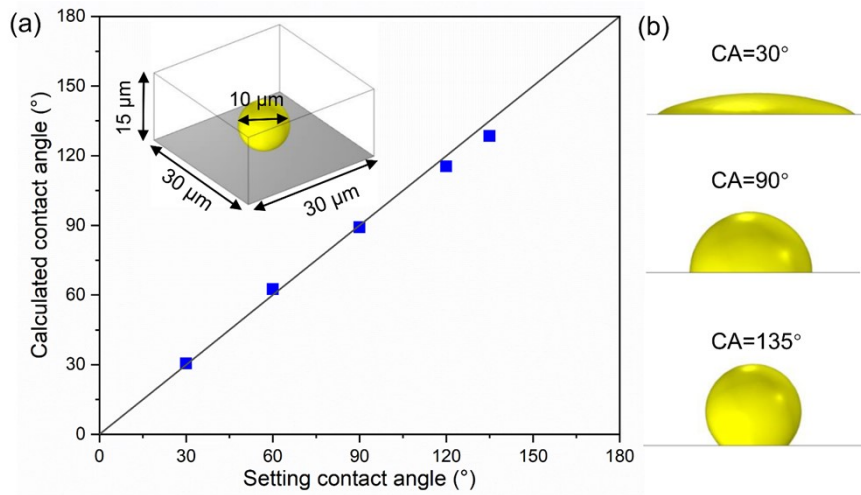


Figure S1. simulation of wetting behavior of underwater oil droplets on a flat surface: (a) calculated contact angles as a function of the setting contact angles; (b) snapshots of oil droplets on the flat surface with setting contact angles of 30°, 60°, 135°.

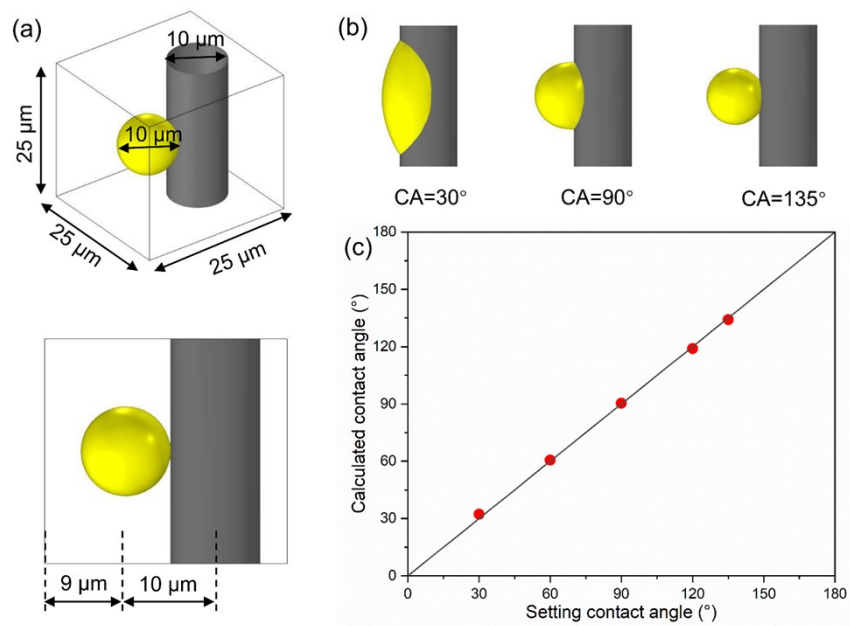


Figure S2. Simulation of wetting behavior of an underwater oil droplet on a cylinder: (a) computational domains of simulation models; (b) snapshots of an oil droplet on the cylinder with setting contact angles of 30°, 60°, 135°; (c) relationship between the calculated contact angles and the setting contact angles of an oil droplet on the cylinder.

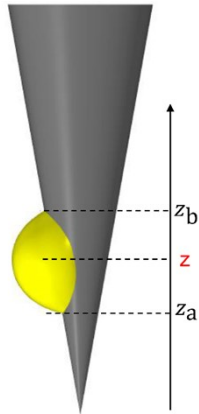


Figure S3. The definition of the center position of the droplet on the cone.

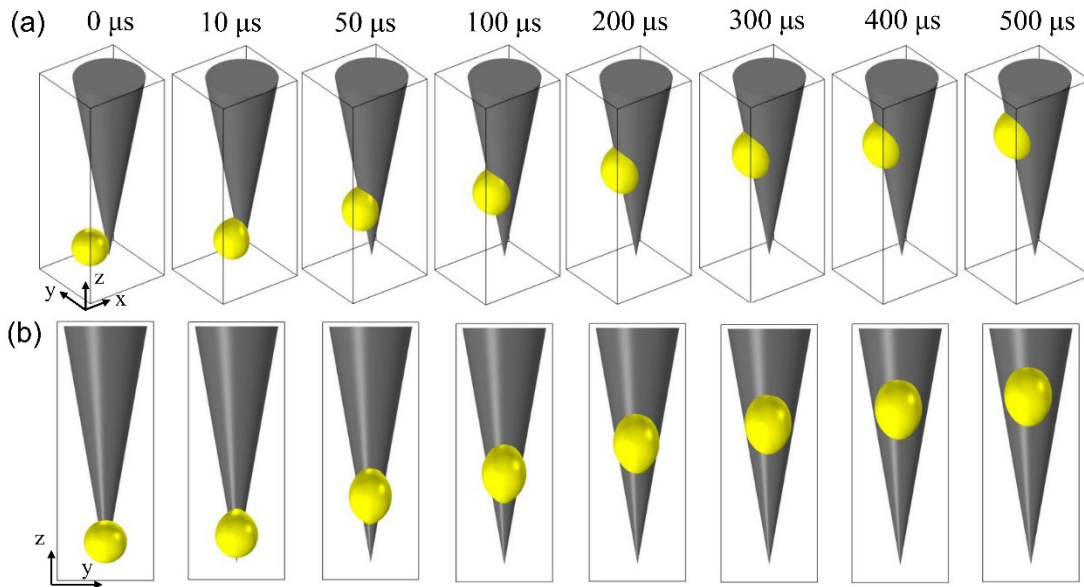


Figure S4. Snapshots of droplet spontaneous motion on the cone in (a) perspective view and (b) y-z view. Parameters: droplet with a diameter of $10\ \mu\text{m}$; the cone with an apex angle of 20° and contact angle of 60° .

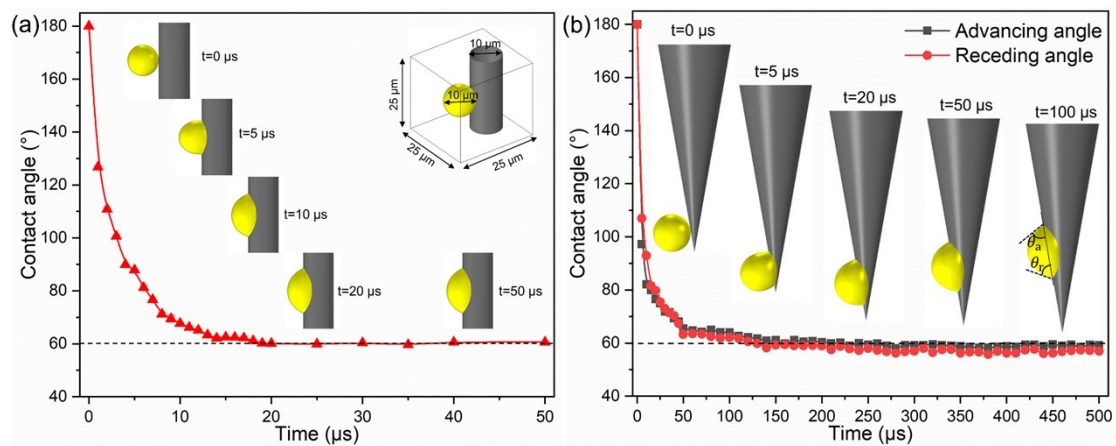


Figure S5. (a) Time-variation of contact angle of oil droplet on the cylinder. (b) Time-variation of contact angle of oil droplet on the cone. (Simulation parameters: setting contact angle: 60° ; droplet diameter: $10\mu\text{m}$; cylinder diameter: $10\mu\text{m}$; apex angle of cone: 20°).

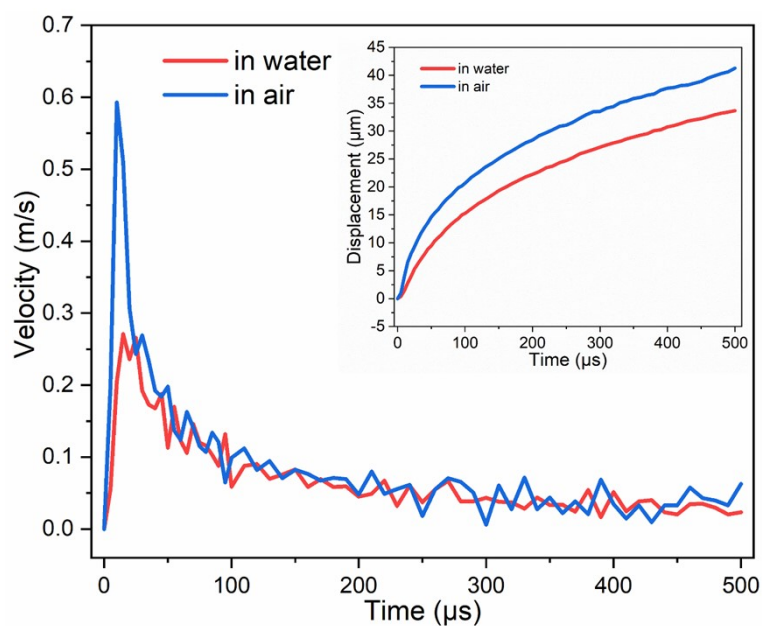


Figure S6. The velocity and displacement of the droplet in water (red line) and in air (blue line) on the cone at same conditions.

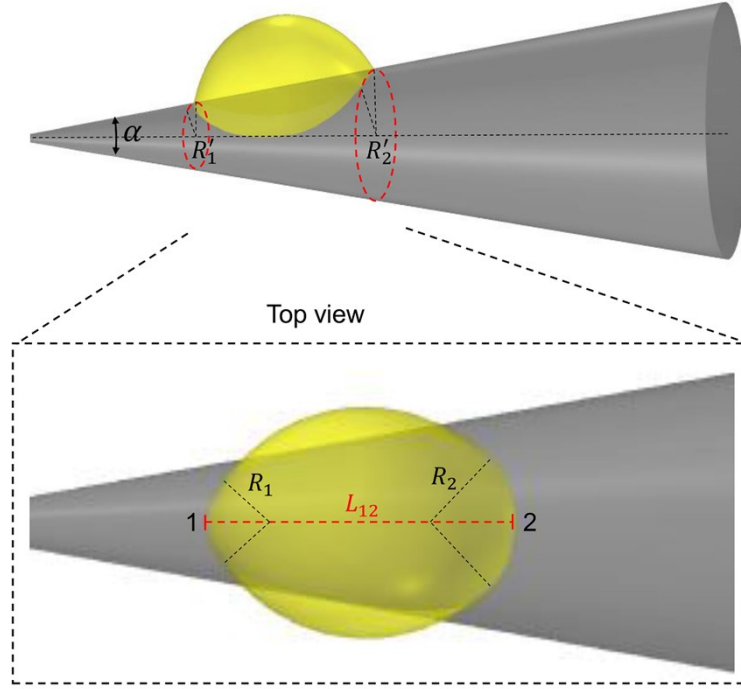


Figure S7. Estimation of the Laplace force induced by curvature gradient when an underwater oil droplet is in clamshell-shaped. The contact area between the oil droplet and cone is a curved surface, which is hard to be depicted. The local contact area can be seen as a flat surface as shown in the top view image. R_1 and R_2 are the local curvature radius of the contact lines at the back and the front side of the droplet. The droplet length (L_{12}) is around $\frac{R_2' - R_1'}{\sin \alpha/2}$. R_1' and R_2' are the cone radii at the back and the front side of the droplet. The different Laplace pressure at back and front of the droplet can be described as $\gamma_{ow}(\frac{1}{R_1} - \frac{1}{R_2})$ and the pressure gradient along the cone can be written as $\gamma_{ow}(\frac{1}{R_1} - \frac{1}{R_2}) \frac{\sin(\alpha/2)}{(R_2' - R_1')}$. For an underwater oil droplet with volume V , the Laplace force acting on the droplet induced by curvature gradient can be estimated

as:

$$F_d \sim \gamma_{ow} \left(\frac{1}{R_1} - \frac{1}{R_2} \right) \frac{\sin(\alpha/2)}{(R_2' - R_1')} V$$

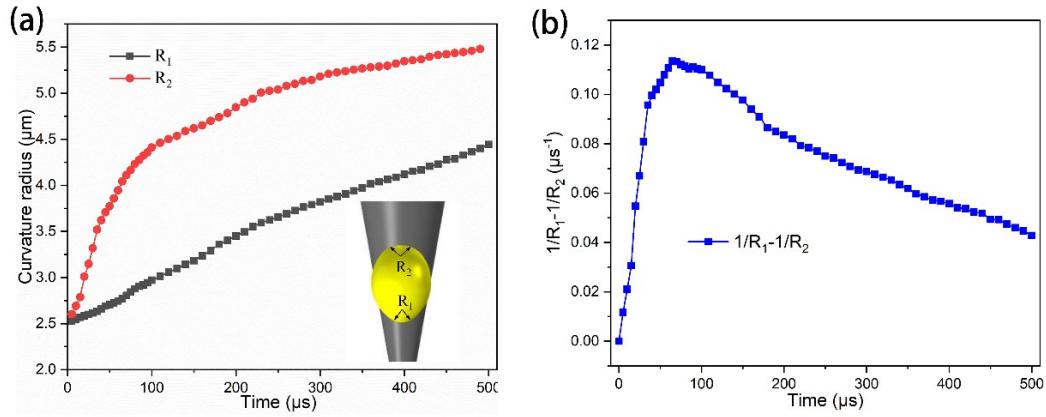


Figure S8. (a) the variation of the curvature radius of the droplet on the cone surface over time. (b) the value of $(1/R_1 - 1/R_2)$ changes over time.

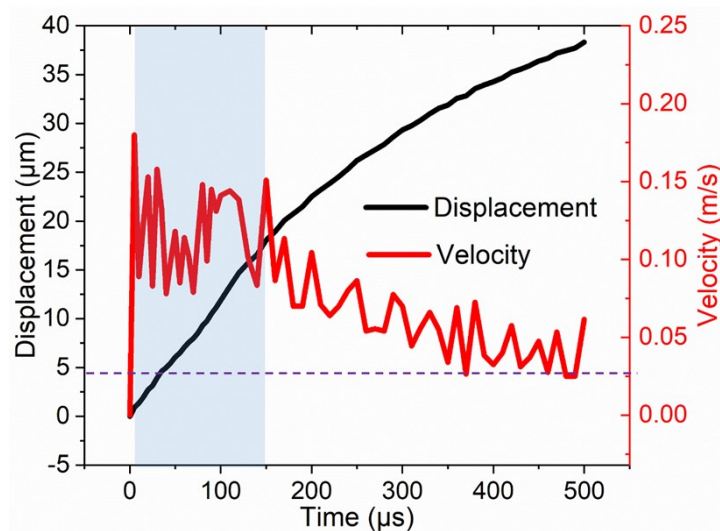


Figure S9. the variation of droplet displacement and velocity in the z-direction with time ($d=10 \mu\text{m}$, $\alpha=10^\circ$, and $\text{CA}=60^\circ$).

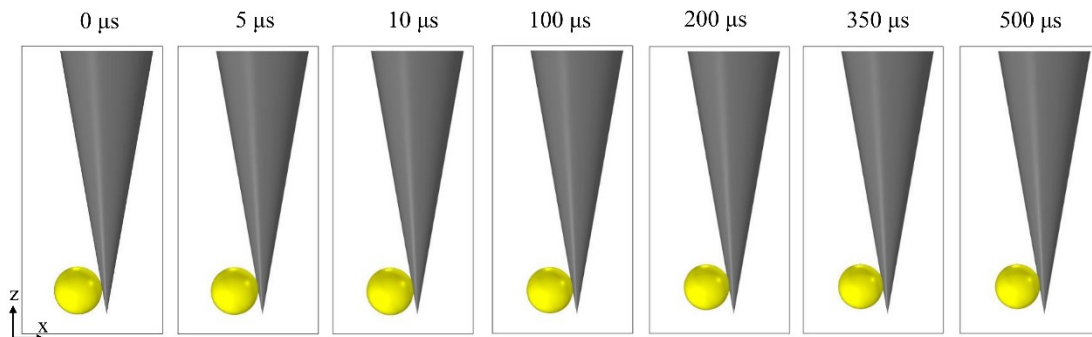


Figure S10. Snapshots of the droplet on the cone with a contact angle of 135° . The droplet was pinned on the initial position and did not move along the cone.

Parameters: droplet diameter: $10 \mu\text{m}$; apex angle of cone: 20° .

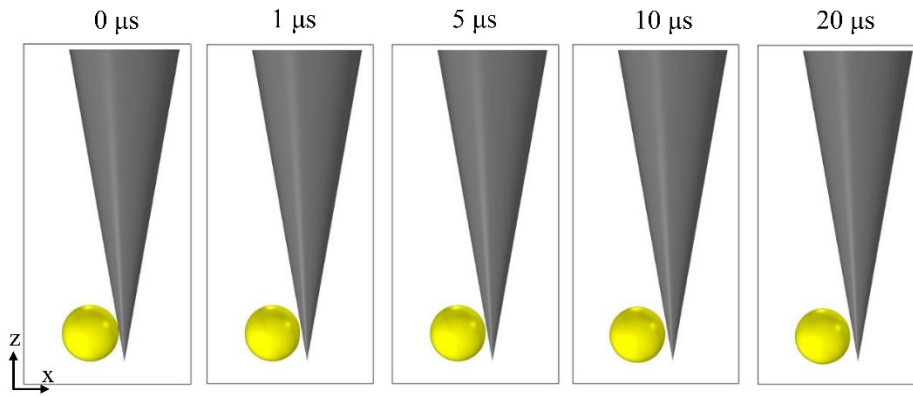


Figure S11. Snapshots of the droplet on the cone with a contact angle of 150° . The droplet would directly detach from the cone. Parameters: droplet diameter: $10\ \mu\text{m}$; apex angle of cone: 20° .

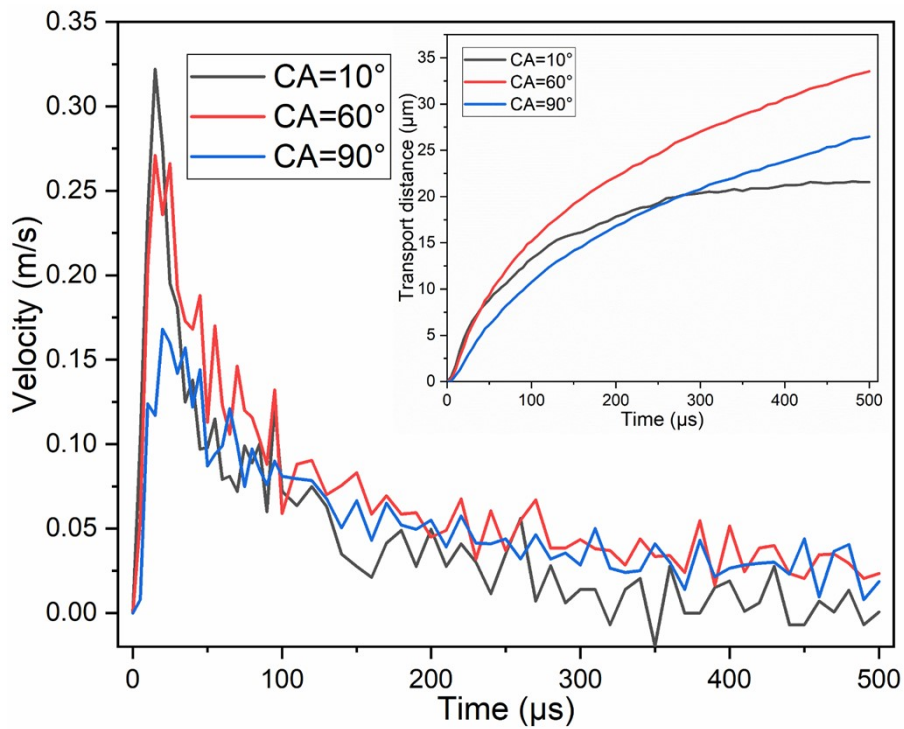


Figure S12. The velocity variation of the droplet on the cone with different contact angles (10° , 60° , 90°) over time. The inset shows the corresponding displacement variation of the droplet on the cone over time.

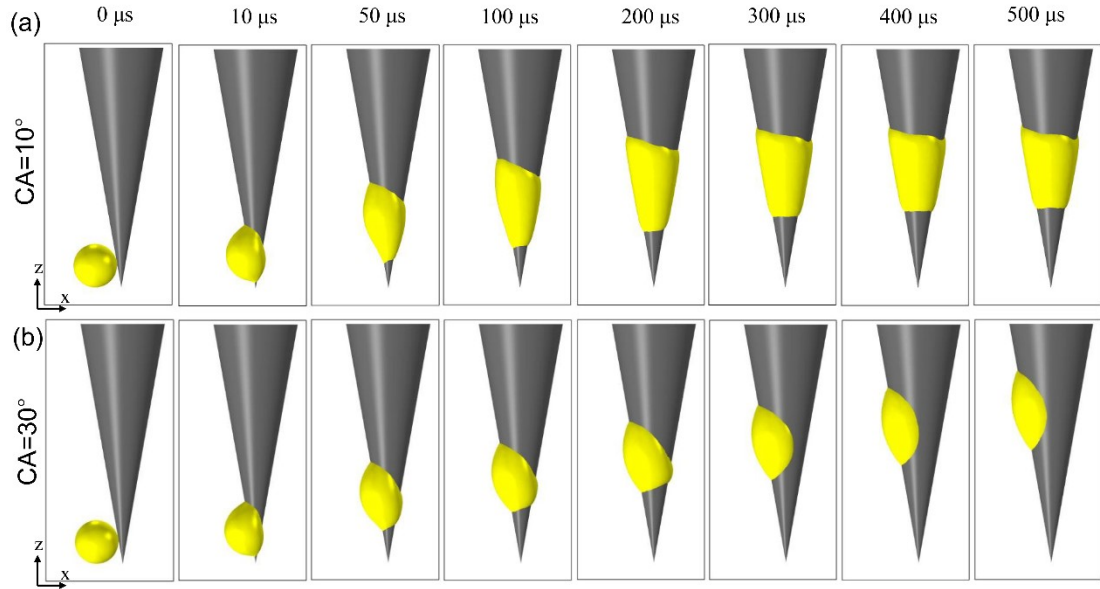


Figure S13. Snapshots of the droplet on the cone with different contact angles (a) 10° and (b) 30° . Parameters: droplet diameter: $10\ \mu\text{m}$; apex angle: 20° .

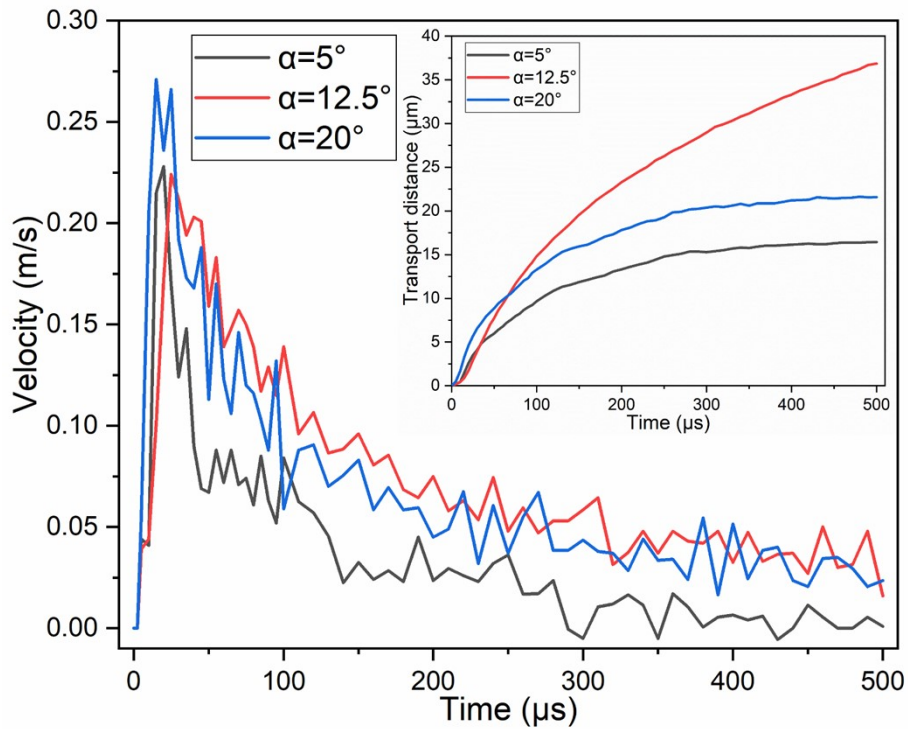


Figure S14. The velocity variation of the droplet on the cone with different apex angles (5° , 12.5° , 20°) over time. The inset shows the corresponding displacement variation of the droplet on the cone over time.

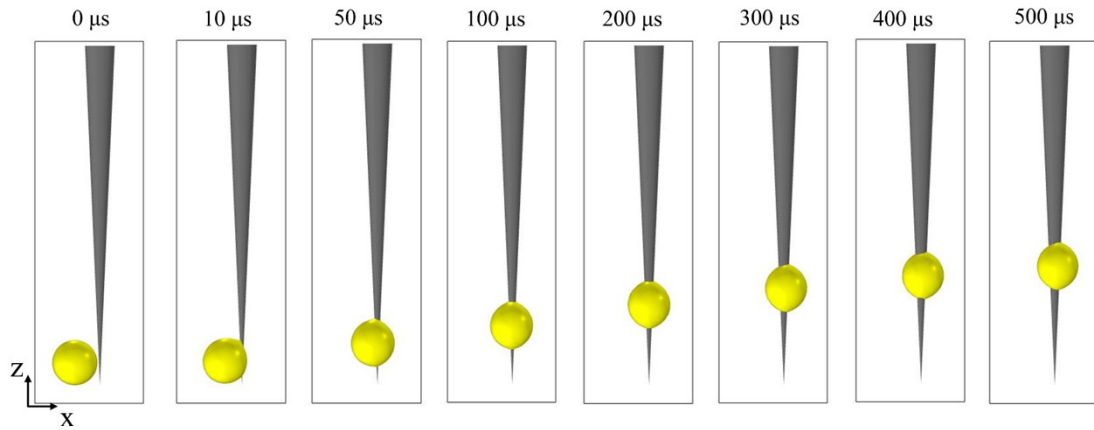


Figure S15. Snapshots of the droplet with a diameter of 10 μm on the cone with contact angles of 60° and apex angle of 5° .

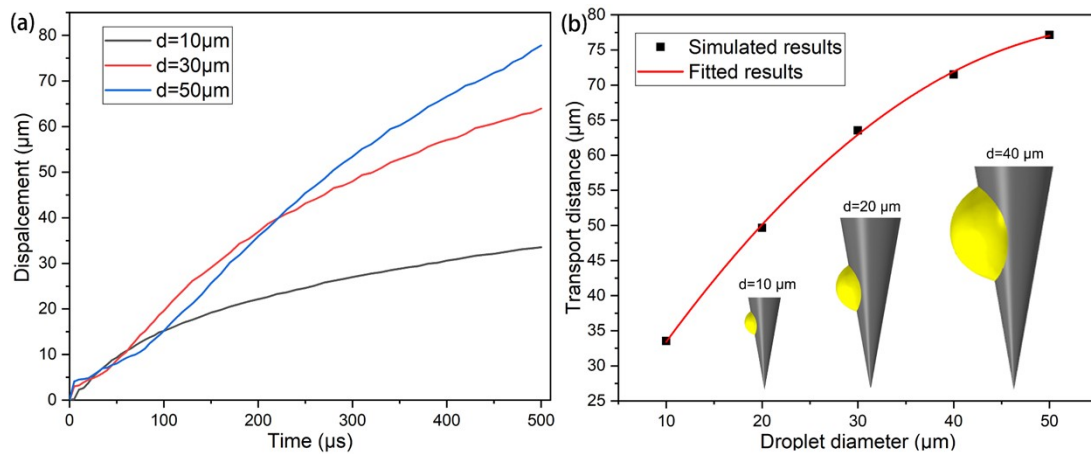


Figure S16. (a) Displacement variation of the droplet with different diameters (10 μm ; 30 μm ; 40 μm) over time. (b) Droplet transport distance on the cone as a function of droplet diameter. The inset represents the droplet position on the cone at 500 μs .